DOI: 10.1002/chem.201001480

Enzymatic Synthesis of Enantiomerically Pure β-Amino Ketones, β-Amino Esters, and β-Amino Alcohols with Baeyer–Villiger Monooxygenases

Jessica Rehdorf,[a] Marko D. Mihovilovic,[b] Marco W. Fraaije,[c] and Uwe T. Bornscheuer*[a]

Abstract: The enzymatic kinetic resolution of a broad set of β-amino ketones was investigated by using a collection of 16 Baeyer–Villiger monooxygenases from different bacterial origins, which display various substrate specificities. Within this platform of enzymes excellent enantioselectivities ($E > 200$) were found towards aliphatic and aromatic 4-amino-2-ketones, and some enzymes even showed opposite enantioselectivity. The intermediate β-aminoalkyl acetates underwent autohydrolysis yielding optically pure β-amino alcohols, which are key intermediates in the synthesis of natural products and bioactive compounds of high interest for the pharmaceutical industry. Furthermore, in some cases the abnormal esters were formed.

Keywords: amino alcohols · amino ketones · Baeyer–Villiger monooxygenases · enantioselectivity · kinetic resolution

Introduction

Biotransformations have become a frequently applied strategy in synthetic routes owing to the advantages of enzyme-mediated conversions, which are usually highly stereospecific and compatible with the concepts of green and sustainable chemistry. Among oxygenation processes the Baeyer–Villiger reaction is one of the most powerful and widely appreciated tools used in synthetic chemistry today.[1–3] The chemical reaction was discovered more than 100 years ago by Adolf Baeyer and Victor Villiger[4] and describes the oxygen insertion process into a carbon–carbon bond with strict retention of configuration. With the discovery of the first Baeyer–Villiger monooxygenase (BVMO) in 1948,[5] nature's enzymatic equivalent of the chemical Baeyer–Villiger oxidation was found. Compared with metal-based mediated catalytic strategies,[6,7] key advantages of enzymatic-driven Baeyer–Villiger reactions are chemo-, regio-, and stereoselectivity combined with the utilization of cheap and safe molecular oxygen as primary oxidant. Recent advances in molecular biology accelerated exploration and investigation of new BVMOs and offered possibilities to modify and optimize the performance of a biocatalytical entity.[8–11] Therefore, the number of recombinantly available BVMOs has heavily increased during the last years, leading to an enzyme platform with a large variety of substrate specificities and complementary properties.[12,13] The most intensively studied BVMO is the cyclohexanone monooxygenase from *Acinetobacter calcoaceticus* NCIMB 9871[14] with over 100 substrates reported,[15,16] illustrative of a broad substrate profile including desymmetrization of prochiral ketones, enantiodivergent reactions, and kinetic resolutions.[13,16] The latter reaction is a particularly powerful approach because two chemically different species are generated. Today, cyclic,[15,17–20] aromatic,[21,22] as well as linear aliphatic[23–26] and aryl-aliphatic ketones[21,27,28] are known to be good substrates for BVMOs. Recently, we investigated a set of various linear aliphatic β-hydroxy ketones as substrates in the enzymatic kinetic resolution and regioselective Baeyer–Villiger oxidation by using a collection of several BVMOs originating from different bacterial origin with overlapping substrate specificity;[29,30] note that these enzymes were previously described as mainly cycloketone-converting proteins. We reported that the majority of enzymes showed high activity towards these model substrates to generate optically pure 2-hydroxy alkyl

[a] J. Rehdorf, U. T. Bornscheuer
University of Greifswald, Institute of Biochemistry
Department of Biotechnology & Enzyme Catalysis
Felix-Hausdorff-Str. 4, 17487 Greifswald (Germany)
Fax: (+49) 3834-86-80066
E-mail: uwe.bornscheuer@uni-greifswald.de

[b] M. D. Mihovilovic
Vienna University of Technology
Institute of Applied Synthetic Chemistry
Getreidemarkt 9/163-OC, 1060 Vienna (Austria)

[c] M. W. Fraaije
University of Groningen, Department of Biochemistry
Nijenborgh 4, 9747 AG Groningen (The Netherlands)

acetates, which undergo ester hydrolysis to yield enantiomerically pure 1,2-diols as the final product. The exchange of the hydroxyl group in the beta-position to the carboxylic function into an electronically different and more demanding amino group followed by subsequent kinetic resolution would consequently lead to β-amino alcohols after cleavage of the β-aminoalkyl acetate intermediate. Furthermore, hydrolysis of the "abnormal" ester, which is formed owing to a different regioselectivity of the enzymes, leads to the formation of N-protected β-amino acids.[31]

Enantiomerically pure β-amino alcohols play an increasingly important role in both the treatment of a wide variety of human disorders, for example, ophthalmic diseases, and as chiral auxiliaries in asymmetric carbon–carbon bond formation. The application field of these compounds is wide and ranges from pharmaceutical intermediates, biological buffers, as well as cosmetic ingredients in paintings, coatings, and metalworking fluids. Moreover, the β-amino alcohol motif does not only occur in drugs, such as ephedrine, chloramphenicol or pronethalol, but is also present in, for example, adrenaline and noradrenaline. The importance of enantiomeric purity in pharmaceuticals has been demonstrated by the debilitating and sometimes harmful side-effects caused by the presence of the nontherapeutic enantiomer of an otherwise beneficial drug.

Among the few chemical methods for synthesizing racemic mixtures of β-amino alcohols, enantiomerically pure compounds are available only through the reduction of amino acids or kinetic resolution of racemic mixtures of amino alcohols or aminoalkyl acetates, often requiring expensive metal catalysts. Furthermore, the reduction of amino acids to the corresponding amino alcohols is economically feasible only for the naturally occurring L-amino acids. The only synthetic methodologies available for the direct synthesis of amino alcohols in high yields are the enantioselective amination of chiral epoxides,[32–34] the directed reductive amination of β-hydroxy ketones,[35] the aminoacetoxylation of alkylenes,[36] and the asymmetric hydrogenation or reduction of prochiral β-amino ketones.[37] Although aminolysis of epoxides suffers from the limitations that chiral epoxides are not readily available, are expensive, and that only monosubstituted and *trans*-symmetrically substituted epoxides can be used, metal-based reactions on the other hand require expensive transition-metal elements (rhodium,[38] palladium, or ruthenium) and ligands such as BINAP. Thus far, only a few enzyme-catalyzed methodologies have been described for the synthesis of enantiomerically pure β-amino alcohols. In the late 1990s the protease subtilisin was subjected to the synthesis of peptidyl amino alcohols as potential specific serine proteinase inhibitors.[39] Another enzymatic approach was the synthesis of enantiopure *N*-aryl-β-amino alcohols in the kinetic resolution of racemic acetates with pig liver esterase (PLE) as shown by Sekar et al.[40]

In this work, an efficient approach for the enzymatic synthesis of linear (branched) aliphatic and aryl aliphatic β-aminoalkyl acetates, as well as β-amino alcohols by using racemic N-protected β-amino ketones as starting materials and Baeyer–Villiger monooxygenases as biocatalysts (Scheme 1) is described in detail. Combined with the fact that successful conversions of nitrogen-containing substrates by BVMOs were reported in the literature only in a very limited number of cases,[41] the possibility to form optically active β-amino alcohols through a Baeyer–Villiger oxidation is an ambitious and challenging approach. It highlights the potential of enzymatic oxygen-insertion processes and demonstrates a new application of Baeyer–Villiger monooxygenases in organic chemistry.

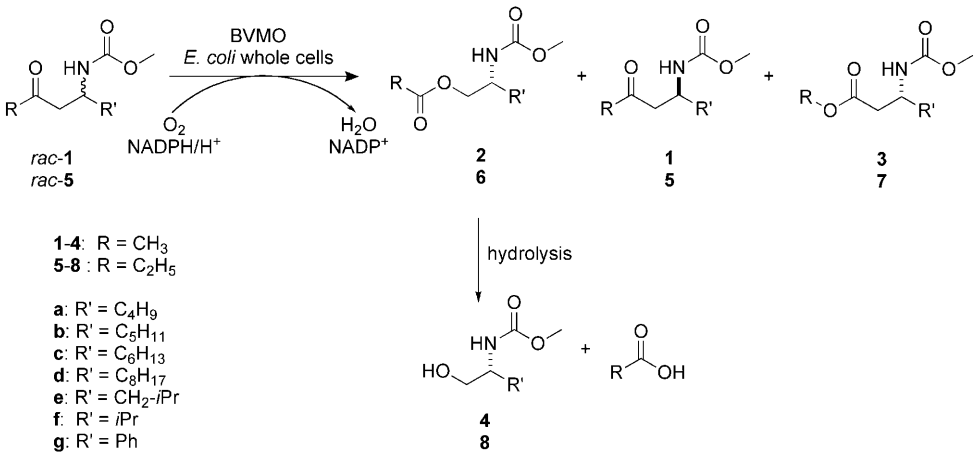

Scheme 1. Kinetic resolution of linear N-protected β-amino ketones by using recombinant Baeyer–Villiger monooxygenases. The enzymatic oxidation yielded primarily the normal ester (**2** or **6**), which underwent hydrolysis to yield the N-protected β-amino alcohols (**4** or **8**). In a few cases (see text) the abnormal esters (**3** or **7**) were also formed.

Results and Discussion

In the present study we utilized a toolbox consisting of 16 BVMOs recombinantly expressed in *Escherichia coli* for the kinetic resolution of β-amino ketones (for further details see the Experimental Section). Among these enzymes ten were revealed to be useful biocatalysts for the intended biotransformations, whereas six did not show activity against the used substrates. Racemic linear aliphatic N-protected β-amino ketones **1a**,**c–g**, **5a**,**b** and **5e** were synthesized by an aza-Michael addition with methylcarbamate as the nitrogen donor[42] from the corresponding α,β-unsaturated ketones generated by an aldol-addition reaction.[43] Enzymatic kinetic resolution was performed as outlined in Scheme 1 by

using *E. coli* cells that had a plasmid with the respective BVMO gene.

The utilization of whole cells, expressing the desired BVMO, compared with isolated enzymes offers highly productive and "easy to handle" biocatalysts[44] combined with the advantages of endogenous cofactor regeneration, increased biocatalyst stability, and renunciation of work-intensive enzyme purification. BVMO-mediated kinetic resolution was initially performed on a screening scale by using 24-well microplates in parallel format.[45] On the basis of these screening results, individual biotransformations were conducted as time-course experiments with selected biocatalysts to investigate the relationship between time, conversion, and enantiomeric excess in detail. For all substrates biotransformations were also performed in preparative scale in baffled shake flasks. Here, a higher oxygen input combined with a better substrate uptake due to a larger surface and an efficient distribution resulted in higher conversions in some cases.

Table 1 summarizes the results from the pre-screening experiments with whole cells expressing $CHMO_{Acineto}$, $CHMO_{Arthro}$, $CHMO_{Brachy}$, $CHMO_{Xantho}$, $CHMO_{Rhodo1}$, $CHMO_{Rhodo2}$, $CHMO_{Brevi1}$, CDMO, $HAPMO_{ACB}$, and PAMO by using **1a**, **1c**–**g**, **5a**, **5b**, and **5e** as substrates.

In principle, five different substrate structures can be distinguished: 1) linear aliphatic 4-amino-2-ketones (**1a**, **1c**, **1d**); 2) linear-branched aliphatic 4-amino-2-ketones (**1e**, **1f**); 3) linear aliphatic 5-amino-3-ketones (**5a**, **5b**); 4) linear-branched aliphatic 5-amino-3-ketones (**5e**); and 5) aryl-aliphatic 4-amino-2-ketones (**1g**). Comparing the results of the type 1 substrates, it becomes obvious that all cyclohexanone-accepting enzymes ($CHMO_{Acineto}$, $CHMO_{Arthro}$, $CHMO_{Brachy}$, $CHMO_{Xantho}$, $CHMO_{Rhodo1}$, $CHMO_{Rhodo2}$) preferentially convert middle-chain 4-amino-2-ketones. Although **1a** (C_8) is converted by all CHMOs with moderate to high enantioselectivities, conversion decreases dramatically with **1d** (C_{12}). Here, $CHMO_{Acineto}$, $CHMO_{Rhodo1}$, and $CHMO_{Rhodo2}$ showed no activity. Presumably, **1d** is too bulky and cannot enter the active site. On the contrary, $HAPMO_{ACB}$ and CDMO revealed a complementary trend. Although conversion for **1a** does not exceed 14% for $HAPMO_{ACB}$, **1c** and **1d** are converted much better (74 and 83% conversion, respectively). This is supported by earlier observations that both enzymes preferentially convert structurally more demanding ketones.[19,27] Nevertheless, chain-length variation does not seem to influence selectivity, because *E* values for all three substrates and both enzymes remain rather poor. Investigating oxidation of **1a** in detail revealed that several BVMOs ($CHMO_{Arthro}$, $CHMO_{Brachy}$, $CHMO_{Xantho}$) convert this compound in an enantiocomplementary way. Thus, implementing $CHMO_{Brachy}$ and $CHMO_{Brevi1}$ in a kinetic-resolution approach would give access to either the *R* or *S* enantiomer of the substrate and product, both in high optical purity.

For type 2 substrates **1e** and **1f**, the problem of steric hindrance is even more prominent. In contrast to type 1 compounds, all BVMOs show moderate to high activity (conversion up to 95%, Table 1), although enantioselectivity is rather poor. Nonetheless, **1e** still appears to be preferred to **1f**. This might be explained by the location of the *i*Pr group in vicinity to the carbonyl function. Although for **1e** the *i*Pr group is more distant owing to an additional $-CH_2$ group, **1f** seems to be more compact. Probably, the proximity of the large terminal substitutent to the reacting center may impede proper positioning of **1f** for catalysis. Thus, all cyclohexanone-converting BVMOs showed a reduced activity towards **1f**, in some cases even 20-fold lower (compare $CHMO_{Acineto}$ in Table 1). On the other hand, $HAPMO_{ACB}$ and CDMO again showed different results, which are consistent with those of **1a**, **1c**, and **1d**. Although **1e** is not converted at all by $HAPMO_{ACB}$, **1f** seemed to be a rather good substrate because conversion reached 41%. A similar effect was observed with CDMO in which conversion increased twofold from **1e** to **1f** (45 and 92%, respectively). Furthermore, note that with the exception of $CHMO_{Brevi1}$ all other BVMOs oxidized the opposite enantiomers compared to **1e** and **1f**. Although for **1e** the (−)-enantiomer is converted, for **1f** the (+)-enantiomer is preferred in all cases except $CHMO_{Brevi1}$, which again oxidized the (−)-enantiomer. This fact might also be connected to the structural difference of both compounds. It is interesting that within this type of substrate $CHMO_{Brevi1}$ displays an enantiocomplementary behavior compared with the other members of the BVMO collection studied. On the bases of protein sequences and biocatalytical performance all cyclohexanone- and cyclopentanone-converting enzymes described so far can be clustered into two groups,[48] giving access to antipodal lactones or esters. Note that $CHMO_{Brevi1}$ clearly possesses a borderline position and this behavior confirms previous observations.[49]

Similar results were obtained for the structurally more demanding type 3 and 4 compounds in which the carbonyl function is shifted further into the center of the molecule. For **5a** and **5b** only CDMO and $HAPMO_{ACB}$ showed activity, whereas **5e** was also accepted by $CHMO_{Arthro}$, $CHMO_{Brachy}$ and $CHMO_{Xantho}$. Interestingly, the formation of the two regioisomers **6e** and **7e** in high optical purity was observed only for **5e**. Here, either the more- or the less-substituted carbon center undergoes migration, leading to the "normal" and "abnormal" ester, respectively. Such regiodivergent biotransformations have been observed in previous studies on linear[29] and (fused) cyclic ketones.[40–55] For the other two substrates, **5a** and **5b**, maximum yield of the abnormal ester did not exceed 5%. Because the formation of regioisomeric esters is less likely when using a chemical Baeyer–Villiger oxidation, it underscores the powerful capabilities of BVMOs and broadens their synthetic applicability in organic chemistry. Besides its high regioselectivity also note that CDMO oxidized the opposite enantiomer of **5e** to give the abnormal product **7e** compared with the cyclohexanone-converting BVMOs $CHMO_{Arthro}$, $CHMO_{Brachy}$, and $CHMO_{Xantho}$, which only generated (−)-**7e** (Table 1). Additionally, upscaling the reaction (0.25 mmol substrate) and performing the biotransformation in a baffled shake flask (500 mL) even increased conversion of **5e** with CDMO

Table 1. Multi-well plate screening of N-protected β-amino ketones with recombinant *E. coli* strains expressing Baeyer–Villiger monooxygenases of various bacterial origin.[a]

Ketone	Ester		Acineto	Arthro	Brachy	Xantho	Rhodo1	Rhodo2	Brevi1	CDMO	$HAPMO_{ACB}$	PAMO
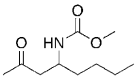 1a	**2a**	% c[b]	35	58	53	64	45	42	37	50	14	26
		% ee_S[c]	52	>99	>99	>99	79	69	58	79	<1	22
		opt. $rot._S$ [d]	(+)	(−)	(−)	(−)	(+)	(+)	(+)	(+)	n.a.	(+)
		% ee_P[c]	96	73	89	57	95	95	>99	80	2	64
		opt. $rot._P$ [d]	(−)	(+)	(+)	(+)	(−)	(−)	(−)	(−)	n.a.	(−)
		E[e]	82	45	116	24	94	80	>200	21	1	6
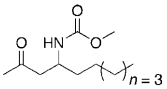 1c	**2c**	% c[b]	3	28	16	17	8	5	30	81	74	traces
		% ee_S[c]	3	39	19	20	8	5	41	>99	27	traces
		opt. $rot._S$[d]	(+)	(+)	(+)	(+)	(+)	(+)	(+)	(+)	(−)	traces
		% ee_P[c]	>99	>99	>99	>99	>99	>99	>99	24	10	traces
		opt. $rot._P$[d]	(−)	(−)	(−)	(−)	(−)	(−)	(−)	(−)	(+)	traces
		E[e]	>200	>200	>200	>200	>200	>200	>200	9	2	traces
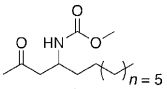 1d	**2d**	% c[b]	n.c.	4	3	17	n.c.	n.c.	20	87	83	n.c.
		% ee_S[c]	n.c.	4	3	20	n.c.	n.c.	25	>99	3	n.c.
		opt. $rot._S$[d]	n.c.	(+)	(+)	(+)	n.c.	n.c.	(+)	(+)	(+)	n.c.
		% ee_P[c]	n.c.	>99	>99	>99	n.c.	n.c.	>99	15	9	n.c.
		opt. $rot._P$[d]	n.c.	(−)	(−)	(−)	n.c.	n.c.	(−)	(−)	(−)	n.c.
		E[e]	n.c.	>200	>200	>200	n.c.	n.c.	>200	7	1	n.c.
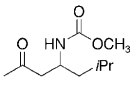 1e	**2e**	% c[b]	44	96	80	95	67	63	31	45	n.c.	traces
		% ee_S[c]	45	>99	>99	>99	>99	98	9	56	n.c.	traces
		opt. $rot._S$[d]	(+)	(+)	(+)	(+)	(+)	(+)	(+)	(+)	n.c.	traces
		% ee_P[c]	57	4	26	5	49	57	21	68	n.c.	traces
		opt. $rot._P$[d]	(−)	(−)	(−)	(−)	(−)	(−)	(−)	(−)	n.c.	traces
		E[e]	6	4	10	4	14	15	2	9	n.c.	traces
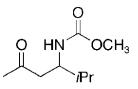 1f	**2f**	% c[b]	2	66	25	43	15	13	4	92	41	traces
		% ee_S[c]	2	98	14	39	13	10	4	54	3	traces
		opt. $rot._S$[d]	(−)	(−)	(−)	(−)	(−)	(−)	(+)	(−)	(−)	traces
		% ee_P[c]	67	52	43	53	71	67	97	5	6	traces
		opt. $rot._P$[d]	(+)	(+)	(+)	(+)	(+)	(+)	(−)	(+)	(+)	traces
		E[e]	6	13	3	5	8	6	68	2	1	traces
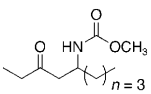 5a	**6a**	% c[b]	n.c.	traces	traces	traces	n.c.	n.c.	n.c.	12	28	n.c.
		% ee_S[c]	n.c.	traces	traces	traces	n.c.	n.c.	n.c.	13	2	n.c.
		opt. $rot._S$[d]	n.c.	traces	traces	traces	n.c.	n.c.	n.c.	(+)	(+)	n.c.
		% ee_P[c]	n.c.	traces	traces	traces	n.c.	n.c.	n.c.	>99	6	n.c.
		opt. $rot._P$[d]	n.c.	traces	traces	traces	n.c.	n.c.	n.c.	(−)	(−)	n.c.
		E[e]	n.c.	traces	traces	traces	n.c.	n.c.	n.c.	>200	1	n.c.
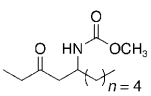 5b	**6b**	% c[b]	n.c.	traces	traces	traces	n.c.	n.c.	n.c.	32	26	n.c.
		% ee_S[c]	n.c.	traces	traces	traces	n.c.	n.c.	n.c.	42	3	n.c.
		opt. $rot._S$[d]	n.c.	traces	traces	traces	n.c.	n.c.	n.c.	(+)	(+)	n.c.
		% ee_P[c]	n.c.	traces	traces	traces	n.c.	n.c.	n.c.	87	9	n.c.
		opt. $rot._P$[d]	n.c.	traces	traces	traces	n.c.	n.c.	n.c.	(−)	(−)	n.c.
		E[e]	n.c.	traces	traces	traces	n.c.	n.c.	n.c.	22	1	n.c.
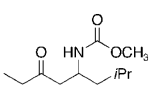 5e	**6e**	% c[b]	n.c.	24	7	13	n.c.	n.c.	n.c.	10	n.c.	n.c.
		% ee_S[c]	n.c.	31	7	15	n.c.	n.c.	n.c.	11	n.c.	n.c.
		opt. $rot._S$[d]	n.c.	(+)	(+)	(+)	n.c.	n.c.	n.c.	(+)	n.c.	n.c.
		% ee_P[c]	n.c.	>99	>99	>99	n.c.	n.c.	n.c.	>99	n.c.	n.c.
		opt. $rot._P$[d]	n.c.	n.d.	n.d.	n.d.	n.c.	n.c.	n.c.	(+)	n.c.	n.c.
		E[e]	n.c.	>200	>200	>200	n.c.	n.c.	n.c.	>200	n.c.	n.c.
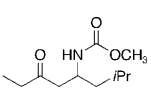 5e	**7e**	% c[b]	n.c.	24	7	13	n.c.	n.c.	n.c.	10	n.c.	n.c.
		% ee_S[c]	n.c.	31	7	15	n.c.	n.c.	n.c.	11	n.c.	n.c.
		opt. $rot._S$[d]	n.c.	(+)	(+)	(+)	n.c.	n.c.	n.c.	(+)	n.c.	n.c.
		% ee_P[c]	n.c.	>99	>99	>99	n.c.	n.c.	n.c.	>99	n.c.	n.c.
		opt. $rot._P$[d]	n.c.	(−)	(−)	(−)	n.c.	n.c.	n.c.	(+)	n.c.	n.c.
		E[e]	n.c.	>200	>200	>200	n.c.	n.c.	n.c.	>200	n.c.	n.c.

Table 1. (Continued)

Ketone	Ester		Acineto	Arthro	Brachy	Xantho	Rhodo1	Rhodo2	Brevi1	CDMO	$HAPMO_{ACB}$	PAMO
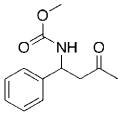	**2g**	% c[b]	75	100	100	100	82	73	15	69	n.c.	51
		% ee_S[c]	70	<1	<1	<1	>99	78	17	63	n.c.	>99
		opt. $rot._S$[d]	(+)	n.a.	n.a.	n.a.	(+)	(+)	(+)	(+)	n.c.	(−)
		% ee_P[c]	24	2	2	5	22	30	>99	29	n.c.	97
		opt. $rot._P$[d]	(−)	(−)	(−)	(−)	(−)	(−)	(−)	(−)	n.c.	(+)
1g		E[e]	3	1	1	1	9	4	>200	3	n.c.	>200

[a] Biotransformations were carried out at 24°C and were monitored over 24 h. Chemical syntheses of β-amino ketones and the enzymatic syntheses of β-amino esters as standards for GC analysis, as well as spectral data of all new compounds, are described and given in the Experimental Section (opt. rot. = optical rotation of substrate (S) or product (P); n.c. = no conversion; n.a. = not applicable; n.d. = not determined). [b] Conversion calculated from the % ee_S (enantiomeric excess of substrate) and % ee_P (enantiomeric excess of product). [c] The % ee_S and % ee_P were determined by chiral-phase GC and calculated according to Chen et al.[46] [d] The sign of optical rotation is given in parentheses. [e] The enantioselectivity values were determined by computer fitting[47] of GC data from the % ee_S and % ee_P.

from 9 to 20% (Table 3), probably due to a better substrate distribution and a higher oxygen input compared to reactions in 24-well microplates.[31]

By using **1g** as the only investigated aryl aliphatic substrate high activity for most of the BVMOs was revealed. Surprisingly, $HAPMO_{ACB}$ showed no conversion, although this enzyme is known to react preferentially with aromatic and aryl aliphatic ketones. Nevertheless, PAMO, also an aryl aliphatic-converting BVMO,[56] proved to be highly selective against **1g**. Even conversion totally stopped at 50%, whereas for the other BVMOs it seemed that the preferred enantiomer is only converted with a slightly higher rate than the nonpreferred enantiomer, resulting in poor enantioselectivities. Furthermore, PAMO generated the enantiocomplementary product compared with cycloketone-converting enzymes.

To optimize enantiomeric excess for all possible products, time-course experiments were performed. Here, samples were taken at different time intervals and conversions were stopped around 50%, when ideally only one substrate enantiomer is converted by a highly selective enzyme. For these experiments, selected biocatalysts were used that showed satisfactory results in prescreening experiments described above. The results of these biotransformations are shown in Figure 1 and all relevant data are compiled in Table 2. The best results for type 1 substrates **1a**, **1c**, and **1d** were achieved by using $CHMO_{Brevi1}$ (E values >200), but also $CHMO_{Brachy}$, $CHMO_{Arthro}$, and $CHMO_{Rhodo1}$ produced excellent enantiomeric excesses (>80% ee) and selectivities. Even after 48 h the less-favored enantiomer is not converted at all by $CHMO_{Brevi1}$ and the reaction stopped at 50%. In comparison, CDMO and $HAPMO_{ACB}$, respectively, oxidized **1c** and **1d** very quickly (less than 10 h for 50% conversion, data not shown), but this was accompanied with a loss of enantioselectivity because the E values were not higher than 13 (Table 2). Performing time-course experiments with **1e** showed an increased enantioselectivity by using $CHMO_{Rhodo1}$ and $CHMO_{Rhodo2}$. When conversion was stopped around 60% the enantiomeric excess of the product enhanced slightly from 57 to 71% ee_P for $CHMO_{Rhodo2}$, suggesting that the (+)-enantiomer is only insignificantly more quickly oxidized compared with the (−)-enantiomer.

Table 2. Microbial Baeyer–Villiger oxidations of the N-protected β-amino ketones **1a** and **1c–g** by using recombinant whole cells of *E. coli* expressing BVMOs of different bacterial origin.[a]

Ester formed	BVMO	t [h]	Conversion [%][b]	ee_S[c] [%]	ee_P[c] [%]	E[d]
2a	Arthro	6	44	72	92 (+)	51
	Rhodo1	42	53	>99	87 (−)	106
	Rhodo2	24	49	88	93 (−)	80
	Xantho	6	52	89	83 (+)	31
	Brevi1	42	51	97	95 (−)	164
	Brachy	6	41	68	98 (+)	>200
2c	Arthro	168	47	90	>99 (−)	>200
	CDMO	6	45	61	76 (−)	13
	Brevi1	168	21	27	99 (−)	>200
	Xantho	20	17	20	>99 (−)	>200
2d	CDMO	8	25	34	>99 (−)	>200
	$HAPMO_{ACB}$	6	42	58	35 (−)	3
	Brevi1	20	50	>99	>99 (−)	>200
2e	Rhodo1	20	61	>99	61 (−)	27
	Rhodo2	20	58	99	71 (−)	29
2f	Arthro	5	27	36	>99 (+)	>200
	$HAPMO_{ACB}$	20	28	35	91 (+)	33
2g	PAMO	6	50	>99	>99 (+)	>200
	Brevi1	120	32	48	>99 (−)	>200

[a] Biotransformations were carried out at 24°C in 24-well plates and monitored over 7 days. Samples were taken at defined time intervals. [b] Conversion calculated from % ee_S (enantiomeric excess of substrate) and % ee_P (enantiomeric excess of product). [c] The % ee_S and % ee_P were determined by chiral-phase GC and were calculated according to Chen et al.[46] The sign of the optical rotation is given in parentheses. [d] Enantioselectivity values were determined by computer fitting of GC[47] data from the % ee_S and % ee_P.

On the other hand, investigating the relationship between time and enantiomeric excess of the product of **1f** by using $CHMO_{Arthro}$ revealed that stopping conversion before 50% could lead to an improved enantiomeric excess. After 24 h 66% of **1f** had been oxidized and the enantiomeric excess of the product was rather low (52% ee_P, Table 1), whereas below 50% conversion, enantiomeric excess was much higher (>99% ee_P).

Also linear and linear-branched aliphatic 5-amino-3-ketones were subjected to time-course experiments, but even after 7 days conversion could not be increased further (data not shown). The best results for **5a**, **5b**, and **5e** were obtained with CDMO (Table 1). However, preparative-scale

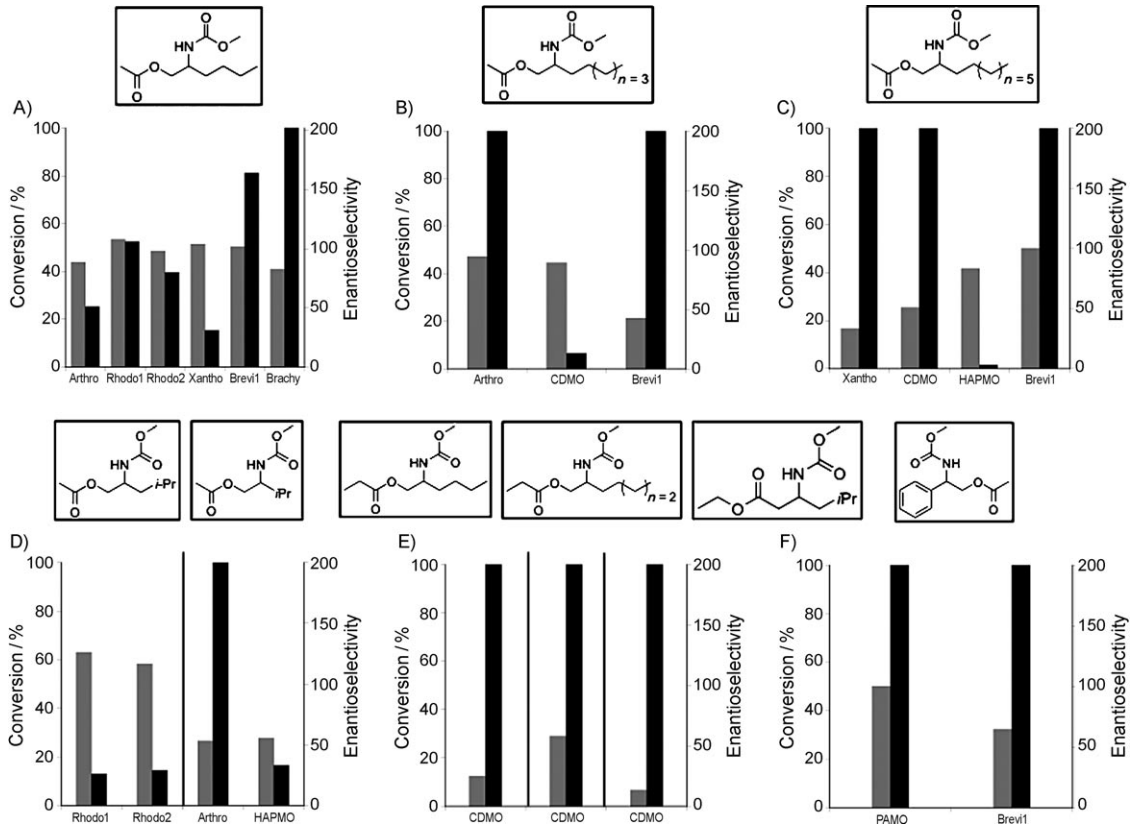

Figure 1. Conversions (grey) and enantioselectivites (black) achieved by using different BVMOs recombinantly expressed in *E. coli* and **1a** (A); **1c** (B); **1d** (C); **1e** and **1f** (D); **5a**, **5b**, and **5e** (E); and **1g** (F) as substrates.

experiments in baffled shake flasks (500 mL) could improve conversions up to threefold without compromising enantioselectivity (Table 3). Obviously, these conditions led to a better substrate distribution and limitations in oxygen input are minimized owing to an increase in surface area, which is necessary for a sufficient cell growth and enzyme activity.

With the exception of $HAPMO_{ACB}$, all other BVMOs oxidized **1g** quite quickly, although time-course experiments did not reveal an increase in selectivity at 50% conversion. Only two enzymes of the collection investigated converted this aryl aliphatic compound in high selectivity. An excellent E value ($E>200$) at a conversion of 33% was obtained with

Table 3. Preparative-scale biotransformation (0.25 mmol substrate) of **5a**, **5b**, and **5e** with CDMO recombinantly expressed in *E. coli*.[a]

Ester	Conversion [%][b]	% ee_S[c]	% ee_P[c]	E[d]
6a	35	54	>99 (−)	>200
6b	41	58	84 (−)	20
7e	20	22	>99 (+)	>200

[a] Preparative biotransformations (0.25 mmol substrate) were carried out at 24 °C. [b] Conversion calculated from % ee_S (enantiomeric excess of substrate) and % ee_P (enantiomeric excess of product). [c] The % ee_S and % ee_P were determined by GC and were calculated according to Chen et al.[46] The sign of the optical rotation is given in parentheses. [d] The enantioselectivity values were determined by computer fitting of GC[47] data from the % ee_S and % ee_P.

$CHMO_{Brevi1}$ after 7 days, suggesting that the **1g**-(−)-enantiomer is not accepted and is therefore not converted. PAMO oxidized **1g** highly selectively with full conversion of the (+)-enantiomer after 6 h, without converting the (−)-enantiomer within the next few days. Thus, utilizing PAMO on one hand would yield the (+)-ester (50% conversion), but using $CHMO_{Brevi1}$ on the other hand gives access to the (−)-ester (32% conversion), both in very high optical purity ($E>200$), as shown in Table 2.

Aligning the crystal structures of PAMO[57] and a cyclohexanone monooxygenase from *Rhodococcus sp.*[58] ($CHMO_{Rhodo3}$), a close homologue of $CHMO_{Rhodo1}$ (protein identity >89%), and performing docking experiments with **1g** revealed a possible reason for PAMO's high enantioselectivity towards only one enantiomer of this substrate. A comparison of the putative binding pockets of both enzymes revealed that in the active site of PAMO an extended loop (PAMO residues 440–446) is in proximity to the reactive peroxy group of the FAD (Figure 2A). In fact, the reduced space due to this stretched loop in PAMO might be the reason that only the (*R*)-enantiomer can be oxidized (based on the computer modeling studies), whereas the (*S*)-enantiomer does not fit properly because of steric hindrance (Figure 2B). In $CHMO_{Rhodo3}$ two additional amino acids are missing (Ser441 and Ala442 in PAMO), which translates into a larger binding pocket, resulting in a rather unselective

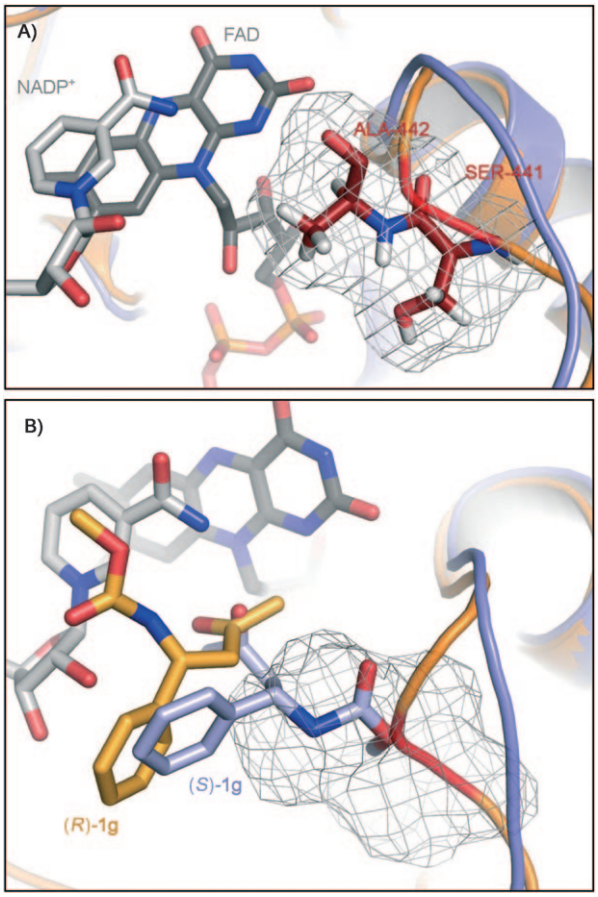

Figure 2. Comparison of both putative binding pockets of PAMO (orange) and CHMO (light blue) from *Rhodococcus sp.* aligned from both crystal structures[57,58] (A) without and (B) with **1g** in both configurations ((*R*)-**1g** is marked in orange, (*S*)-**1g** in light blue). FAD (dark grey) and NADP+ (light grey) are shown as sticks. Residues Ser441 and Ala442 and the backbone amino acid chain are highlighted in red.

conversion of **1g**. Furthermore, the distance between the reaction center of (*R*)-**1g** and the C4a atom of the FAD cofactor is about 4 Å (compared with the (*S*)-enantiomer of 8 Å), which means that the reactive flavin peroxy species is spatially close enough to the carbonyl group of the substrate to perform a Baeyer–Villiger oxidation. The relationship between the loop segment Pro440-Met446 of PAMO and its selectivity was also outlined in previous studies on rational protein design.[10,59–62]

The above is also in line with the observation that CPMO, which also contains a PAMO-like extended loop, does not accept the studied β-amino ketones. A protein sequence alignment of PAMO, CPMO, $CHMO_{Rhodo1}$, and other cyclohexanone monooxygenases that were also subjected to kinetic resolution with N-protected β-amino-4-phenylbutan-2-one, confirms the absence of a PAMO-like extended loop in CHMOs (Figure 3). This is in agreement with the observed poor enantioselectivity of all CHMOs in the oxidation of **1g** (Figure 3).

Kinetic resolution of β-amino ketones can be an attractive tool in organic chemistry because two different optically

```
PAMO          PNLFFIAGPGSPSALSNMLVS
CPMO          PNLLFGYGPQSPAGFCNGPSS
CHMO_Brevi2   PNLMFLYGPQSPSGFCNGTDF
CHMO_HI-31    PNMFMILGPNGP--FTNLPPT
CHMO_Rhodo1   PNWFMVLGPNGP--FTNLPPS
CHMO_Acineto  PNMFMVLGPNGP--FTNLPPS
CHMO_Brevi1   PNFLMSLGPQTP--YSNLVVP
```

Figure 3. Alignment of seven BVMO protein sequences highlighting the loop segment 441–444 (grey box, residues 441 and 442 are written in bold letters), which is closely related to PAMO's enantioselectivity in kinetic resolution of N-protected β-amino-4-phenylbutan-2-one. Code: phenylacetone monooxygenase from *T. fusca* (PAMO: 1wx4), cyclopentanone monooxygenase from *Comamonas sp.* (CPMO: BAC22652), cyclohexanone monooxygenase from *Brevibacterium sp.* HCU (CHMO Brevi2: AAG01290), cyclohexanone monooxygenase from *Rhodococcus sp.* HI-31 (CHMO HI-31: 3GWFA), cyclohexanone monooxygenase from *Rhodococcus sp.* Phi1 (CHMO Rhodo1: AAN57494), cyclohexanone monooxygenase from *A. calcoaceticus* NCIMB 9871 (CHMO Acineto: BAA86293), and cyclohexanone monooxygenase from *Brevibacterium sp.* HCU (CHMO Brevi1: AAG01289).

active species are formed, which additionally differ in their configuration: besides the residual β-amino ketone, a β-aminoalkyl acetate is also generated. Interestingly, this aminoalkyl acetate can undergo autohydrolysis to give enantiomerically pure N-protected β-amino alcohols, which are highly valuable building blocks in the pharmaceutical industry. Because ester hydrolysis proceeds without any configurational changes, the resulting β-amino alcohols possess the same absolute configuration as the aminoalkyl acetates. The maximum amount of generated N-protected β-amino alcohol observed was 56% after 7 days by using **1c** as the starting material and CDMO as the biocatalyst. It seems that with a decrease in pH due to cell metabolism, the ester bond of the Baeyer–Villiger product is cleaved, resulting in the formation of acetic acid and the corresponding β-amino alcohol. For all ketones in which alcohol production was detected (Figure 4), spontaneous ester hydrolysis started 30 h and 42 h, respectively, after substrate addition. This observation makes the kinetic resolution of linear β-amino ketones even more sophisticated because a third interesting, bioac-

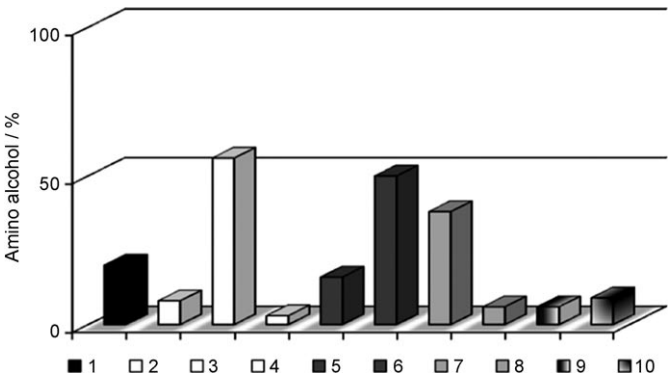

Figure 4. Formation of N-protected 2-amino alcohols after autohydrolysis of corresponding β-amino esters (1 = **4a**, $CHMO_{Arthro}$; 2 = **4c**, $CHMO_{Arthro}$; 3 = **4c**, CDMO; 4 = **4c**, $CHMO_{Brevi1}$; 5 = **4e**, $CHMO_{Rhodo1}$; 6 = **4e**, $CHMO_{Brachy}$; 7 = **4f**, $CHMO_{Arthro}$; 8 = **4f**, $CHMO_{Brachy}$; 9 = **8b**, CDMO; 10 = **8e**, $CHMO_{Arthro}$).

tive, and valuable compound can be generated in high optical purity.

Conclusion

Within these studies we could demonstrate that BVMOs indeed can be a very attractive and useful biocatalytic tool to generate chiral synthons of high interest for the pharmaceutical, food, and synthetic chemical industry. Besides formation of enantiomerically pure linear aliphatic β-aminoalkyl esters and residual β-amino ketones, respectively, they also proved to be capable of allowing access to compounds like β-amino alcohols, which do not belong to the common products usually associated with the enzymatic Baeyer–Villiger oxidation. Similar possibilities have been shown in earlier studies on the hydroxyl counterpart in the beta-position of the carboxylic function.[29] Regarding this potential BVMOs appear to be widely applicable in organic chemistry because they are able to convert substituents with different inductive effects and electronic environments in vicinity to the carboxylic group. Moreover, the majority of investigated BVMOs, which goes along with the majority of recombinantly available BVMOs today, not only accept N-protected β-amino ketones as substrates, but they even oxidize them in a highly selective manner, leading to optically active and enantiocomplementary products. Within the five different structural types of racemic substrates examined in this contribution, the short-chain linear aliphatic 4-amino-2-ketones as well as the aryl-aliphatic amino ketone were revealed to be the best substrates regarding conversion and enantioselectivity. In both cases several BVMOs were identified to yield the opposite enantiomers of product ester and residual ketone. For all other substrates the number of suitable BVMOs decreased, but still certain biocatalysts were found to perform kinetic resolutions enantioselectively. Furthermore, for linear-branched 5-amino-3-ketones it was shown that BVMOs possess a regioselectivity that is not accessible when using the chemical Baeyer–Villiger reaction, leading to the abnormal product in high enantiomeric excess. The excellent enantioselectivity combined with the chemoselectivity and naturally occurring regioselectivity makes the enzymatic Baeyer–Villiger oxidation an essential strategy and method for the synthesis of optically active valuable compounds.

Experimental Section

Chemical synthesis: Unless otherwise stated, all chemicals and microbial growth media were purchased from commercial suppliers and were used without further purification. All solvents were distilled prior to use. Flash column chromatography was performed on silica gel 60 from Merck (40–63 μm). NMR spectra were recorded from $CDCl_3$ solution on a Bruker AC 200 (200 MHz) and chemical shifts are reported in ppm by using TMS as an internal standard. Combustion analysis was carried out in the Microanalytic Laboratory, University of Vienna, whereas mass spectra analysis was performed at the University of Greifswald. Analyses of purified products and sample measurements were performed on a Thermo Focus DSQ (quadrupol, EI+) by using a capillary column BGB5 (5% diphenyl-, 95% dimethylpolysiloxane, 30 m × 0.25 mm ID). Enantiomeric excesses were determined by chiral-phase GC (Thermo Trace and Focus) by using a BGB 175 (2,3-diacetyl-6-*tert*-butyldimethylsilyl-γ-cyclodextrin, 30 m × 0.25 mm ID) or a hydrodex β-TBDAc column (30 m × 0.25 mm ID). Specific optical rotations, $[\alpha]_D^{20}$ were determined by using a Perkin–Elmer Polarimeter 241.

Bacterial strains and growth conditions: *E. coli* that contained the plasmids for the particular BVMOs were routinely cultivated on LB agar (1% bacto peptone, 0.5% bacto yeast extract, 1% NaCl, 1.5% agar) plates supplemented with ampicillin (200 μg mL^{-1}) and stored as frozen stocks (15% glycerol) at −80 °C. Liquid cultures were grown in standard LB media (1% bacto peptone, 0.5% bacto yeast extract, 1% NaCl) supplemented with ampicillin (LB_{amp}) in baffled Erlenmeyer flasks on an orbital shaker (120 rpm at 37 °C).

Substrate synthesis

General procedure for chemical syntheses of linear N-protected β-amino ketones: The synthesis of **1a**, **1c**–**1g**, **5a**, **5b**, and **5e** was performed in two reaction steps: an aldol addition leading to α,β-unsaturated ketones followed by an aza-Michael addition. With the exception of 5-methylhexen-2-one, 3-octen-2-one, 3-decen-2-one, and 4-phenyl-3-buten-2-one, which were commercially available, all other α,β-unsaturated ketones were synthesized by aldol addition as described by Kourouli et al.,[43] purified by vacuum distillation (>99%) or medium-pressure liquid chromatography (MPLC) and used as a starting material in an aza-Michael-addition.[42] Here, methylcarbamate served as the nitrogen donor, tributylphosphine as the catalyst and TMSCl as the reaction starter. All reactions were carried out in dry dichloromethane under vigorous stirring at room temperature or under reflux. After the reaction was completed (usually after 2–7 days, monitored by TLC), the mixture was quenched with saturated sodium bicarbonate and extracted three times with chloroform. The organic layers were combined, dried over anhydrous sodium sulphate, filtered, and the solvent was evaporated. The crude products were purified by using silica-gel chromatography (petrol ether/ethyl acetate: 10:1 or 5:1). Both the linear α,β-unsaturated ketones as well as the N-protected β-amino ketones were identified and analyzed by GCMS and $^1H/^{13}C$ NMR.

Physical and spectral data of chemically synthesized α,β-unsaturated ketones

3-Dodecen-2-one ($C_{12}H_{22}O$): Obtained from ethyl acetoacetate (12.87 g, 0.1 mol) and *n*-decanal (7 g, 0.05 mol) as a colorless liquid (yield: 500 mg, 21%) as described by Kourouli et al.[43]

6-Methyl-3-hepten-2-one ($C_8H_{14}O$): Obtained from ethyl acetoacetate (12.78 g, 0.1 mol) and *iso*-valeraldehyde (4.7 g, 0.05 mol) as a colorless liquid (yield: 4 g, 85%) as described by Kourouli et al.[43]

4-Nonen-3-one ($C_9H_{16}O$): Obtained from ethyl propionylacetate (14 g, 0.1 mol) and *n*-valeraldehyde (4.7 g, 0.05 mol) as a yellowish liquid (yield: 1.5 g, 38%) as described by Kourouli et al.[43]

4-Decen-3-one ($C_{10}H_{18}O$): Obtained from ethyl propionylacetate (14 g, 0.1 mol) and capronaldehyde (5 g, 0.05 mol) as a yellow liquid (yield: 2.5 g, 50%) as described by Kourouli et al.[43]

7-Methyl-4-octen-3-one ($C_9H_{16}O$): Obtained from ethyl propionylacetate (3 g, 0.2 mol) and *iso*-valeraldehyde (1.7 g, 0.2 mol) as a colorless liquid (yield: 1 g, 58%) as described by Kourouli et al.[43]

Physical and spectral data of chemically synthesized N-protected β-amino ketones

*Compound **1a** ($C_{10}H_{19}NO_3$)*: Obtained from 3-octen-2-one (1.5 g, 10 mmol), methylcarbamate (900 mg, 12 mmol), $(n\text{Bu})_3\text{P}$ (250 mg, 1 mmol), and TMSCl (1.4 g, 11 mmol) as a colorless solid. Yield: 920 mg, 51%; m.p. 38–40 °C; specific rotation of sample obtained from enzymatic kinetic resolution: $[\alpha]_D^{20} = +33.4$ ($c = 1.03$ in $CHCl_3$; *ee* = 94%); ^1H NMR (200 MHz, $CDCl_3$, 25 °C, TMS): $\delta = 0.87$ (t, $J = 6.6$ Hz, 3H), 1.21–1.51 (m, 6H), 2.14 (s, 3H), 2.64 (d, $J = 5.4$ Hz, 2H) 3.63 (s, 3H), 3.80–3.97 (m, 1H), 5.01–5.10 ppm (m, 1H); ^{13}C NMR (50 MHz, $CDCl_3$, 25 °C, TMS): $\delta = 13.9$ (q), 22.4 (t), 28.4 (t), 30.5 (q), 34.2 (t), 47.8 (d), 48.0 (t), 51.9 (q), 156.6 (s), 207.8 ppm (s); ESIMS-TOF (70 eV): *m*/*z* (%): 236 (100), [*M*+

$2H_2O-1]^-$, 200 (9) $[M-1]^-$, 193 (9) $[C_8H_{16}NO_2+2H_2O-1]^-$, 182 (50) $[M-H_2O-1]^-$.

Compound ***1c*** *($C_{12}H_{23}NO_3$)*: Obtained from 3-decen-2-one (1.8 g, 10 mmol), methylcarbamate (900 mg, 12 mmol), $(n\mathrm{Bu})_3$P (250 mg, 1 mmol) and TMSCl (1.4 g, 11 mmol) as a colorless solid. Yield: 1.3 g, 61 %; m.p. 50–52 °C; specific rotation of sample obtained from enzymatic kinetic resolution: $[\alpha]_D^{20}=+28.3$ ($c=1.20$ in $CHCl_3$; *ee* = 99 %); ^{1}H NMR (200 MHz, $CDCl_3$, 25 °C, TMS): $\delta=0.88$ (t, $J=7$ Hz, 3H), 1.23–1.61 (m, 10H), 2.15 (s, 3H), 2.65 (d, $J=6$ Hz, 2H), 3.64 (s, 3H), 3.82–3.98 (m, 1H), 5.09–5.18 ppm (m, 1H); ^{13}C NMR (50 MHz, $CDCl_3$, 25 °C, TMS): $\delta=13.9$ (q), 22.5 (t), 26.1 (q), 28.9 (t), 30.5 (t), 31.7 (t), 34.5 (t), 47.9 (d), 48.1 (t), 51.9 (q), 156.6 (s), 207.8 ppm (s); elemental analysis calcd (%) for $C_{12}H_{23}NO_3$: C 62.85, H 10.11, N 6.11; found: C 63.14, H 9.99, N 6.09.

Compound ***1d*** *($C_{14}H_{27}NO_3$)*: Obtained from 3-dodecen-2-one (770 mg, 3 mmol), methylcarbamate (300 mg, 4 mmol), $(n\mathrm{Bu})_3$P (60 mg, 0.3 mmol), and TMSCl (400 mg, 3.7 mmol) as a colorless solid. Yield: 280 mg, 51 %; m.p. 62–64 °C; specific rotation of sample obtained from enzymatic kinetic resolution: $[\alpha]_D^{20}=+7.1$ ($c=0.56$ in $CHCl_3$; *ee* = 30 %); ^{1}H NMR (200 MHz, $CDCl_3$, 25 °C, TMS): $\delta=0.86$ (t, $J=6.6$ Hz, 3H), 1.24–1.48 (m, 14H), 2.14 (s, 3H), 2.64 (d, $J=5.4$ Hz, 2H), 3.63 (s, 3H), 3.83–3.94 (m, 1H), 4.99–5.08 ppm (m, 1H); ^{13}C NMR (50 MHz, $CDCl_3$, 25 °C, TMS): $\delta=14.2$ (q), 22.8 (t), 26.4 (q), 29.3 (t), 29.5 (t), 30.7 (t), 31.9 (t), 34.7 (t), 48.0 (d), 48.2 (t), 52.1 (q), 156.7 (s), 207.3 ppm (s); elemental analysis calcd (%) for $C_{14}H_{27}NO_3$: C 65.33, H 10.43, N 5.44; found: C 66.01, H 10.43, N 5.44.

Compound ***1e*** *($C_{10}H_{19}NO_3$)*: Obtained from 6-methyl-3-hepten-2-one (4 g, 30 mmol), methylcarbamate (2.7 g, 36 mmol), $(n\mathrm{Bu})_3$P (600 mg, 3 mmol), and TMSCl (3.6 g, 33 mmol) as a yellow liquid. Yield: 2.5 g, 52 %; specific rotation of sample obtained from enzymatic kinetic resolution: $[\alpha]_D^{20}=+49.9$ ($c=0.70$ in $CHCl_3$; *ee* = 99 %); ^{1}H NMR (200 MHz, $CDCl_3$, 25 °C, TMS): $\delta=0.89$ (d, $J=6.6$ Hz, 6H), 1.15–1.32 (m, 1H), 1.40–1.1.68 (m, 2H), 2.12 (s, 3H), 2.63 (d, $J=5.4$ Hz, 2H), 3.62 (s, 3H), 3.85–4.08 (m 1H), 5.01–5.11 ppm (m, 1H); ^{13}C NMR (50 MHz, $CDCl_3$, 25 °C, TMS): $\delta=22.1$ (q), 23.1 (q), 25.1 (d), 30.7 (q), 43.7 (d), 46.3 (t), 48.3 (t), 52.1 (q), 156.6 (s), 208.0 ppm (s); ESIMS-TOF (70 eV): *m*/*z* (%): 236 (15) $[M+2H_2O-H]^-$, 182 (7) $[M-H_2O-1]^-$.

Compound ***1f*** *($C_9H_{17}NO_3$)*: Obtained from 5-methyl-3-hexen-2-one (5.6 g, 50 mmol), methylcarbamate (4.5 g, 60 mmol), $(n\mathrm{Bu})_3$P (1.01 g, 5 mmol), and TMSCl (6 g, 55 mmol) as a yellow liquid. Yield: 2.3 g, 34 %; specific rotation of sample obtained from enzymatic kinetic resolution: $[\alpha]_D^{20}=-50.2$ ($c=0.43$ in $CHCl_3$; *ee* = 99 %); ^{1}H NMR (200 MHz, $CDCl_3$, 25 °C, TMS): $\delta=0.91$ (d, $J=6.8$ Hz, 6H), 1.79–1.95 (m, 1H), 2.16 (s, 3H), 2.61 (d, $J=6$ Hz, 2H), 3.63 (s, 3H), 3.69–3.89 (m, 1H), 5.02–5.10 ppm (m, 1H); ^{13}C NMR (50 MHz, $CDCl_3$, 25 °C, TMS): $\delta=18.6$ (q), 19.5 (q), 30.4 (q), 31.8 (d), 45.8 (t), 52.2 (d), 53.5 (q), 156.7 (s), 208.0 ppm (s); ESIMS-TOF (70 eV): *m*/*z* (%): 355 (25) $[2M-H_2O-H]^-$, 337 (20) $[2M-2H_2O-1]^-$, 222 (33) $[M+2H_2O-1]^-$.

Compound ***1g*** *($C_{12}H_{15}NO_3$)*: Obtained from 4-phenyl-3-buten-2-one (1.95 g, 13.3 mmol), methylcarbamate (1.2 g, 16 mmol), $(n\mathrm{Bu})_3$P (270 mg, 1.3 mmol), and TMSCl (1.88 g, 14.7 mmol) as a yellow oil. Yield: 810 mg, 35 %; specific rotation of sample obtained from enzymatic kinetic resolution: $[\alpha]_D^{20}=-11.7$ ($c=1.84$ in $CHCl_3$; *ee* = 87 %); ^{1}H NMR (200 MHz, $CDCl_3$, 25 °C, TMS): $\delta=2.02$ (s, 3H), 2.77–3.05 (dd, $J=16.4$ Hz and 6.6 Hz, 2H), 3.57 (s, 3H), 5.03–5.10 (m, 1H), 5.59–5.68 (m, 1H), 7.05–7.15 ppm (m, 5H); ^{13}C NMR (50 MHz, $CDCl_3$, 25 °C, TMS): $\delta=14.1$ (q), 48.9 (t), 51.4 (d), 52.2 (q), 126.9 (t), 126.9 (t), 128.3 (t), 128.3 (t), 128.6 (t), 141.2 (d), 156.3 (s), 206.8 ppm (s).

Compound ***5a*** *($C_{11}H_{21}NO_3$)*: Obtained from 4-nonen-3-one (1.4 g, 10 mmol), methylcarbamate (900 mg, 12 mmol), $(n\mathrm{Bu})_3$P (202 mg, 1 mmol), and TMSCl (1.2 g, 11 mmol) as a colorless solid: Yield: 568 mg, 34 %; mp: 40–42 °C; specific rotation of sample obtained from enzymatic kinetic resolution: $[\alpha]_D^{20}=+16.8$ ($c=0.37$, $CHCl_3$; *ee* = 54 %); ^{1}H NMR (200 MHz, $CDCl_3$, 25 °C): $\delta=0.85$ (t, $J=6.8$ Hz, 3H), 1.03 (t, $J=7.4$ Hz, 3H), 1.25–1.72 (m, 6H), 2.42 (q, $J=7.4$ Hz, 2H), 2.63 (dd, $J=5.4$ and 2.4 Hz, 2H), 3.64 (s, 3H), 3.81–3.99 (m, 1H), 5.04–5.17 ppm (m, 1H); ^{13}C NMR (50 MHz, $CDCl_3$, 25 °C): $\delta=7.7$ (q), 14.1 (q), 22.6 (t), 28.6 (t), 34.4 (t), 36.7 (t), 46.6 (d), 48.3 (t), 52.1 (q), 156.7 (s), 210.1 ppm (s); combustion analysis or ESI-MS-TOF not applicable.

Compound ***5b*** *($C_{12}H_{23}NO_3$)*: Obtained from 4-decen-3-one (2.46 g, 16 mmol), methylcarbamate (1.44 g, 19 mmol), $(n\mathrm{Bu})_3$P (324 mg, 1.6 mmol), and TMSCl (1.91 g, 17.6 mmol) as a colorless solid. Yield: 1.2 g, 41 %; m.p. 44–46 °C; specific rotation of sample obtained from enzymatic kinetic resolution: $[\alpha]_D^{20}=+23.8$ ($c=0.20$ in $CHCl_3$; *ee* = 58 %); ^{1}H NMR (200 MHz, $CDCl_3$, 25 °C, TMS): $\delta=0.88$ (t, $J=6.6$ Hz, 3H), 1.03 (t, $J=7.2$ Hz, 3H), 1.21–1.75 (m, 8H), 2.42 (q, $J=7.4$ Hz, 2H), 2.62 (dd, $J=5.2$ Hz and 2.8 Hz, 2H), 3.64 (s, 3H), 3.81–3.99 (m, 1H), 5.01–5.13 ppm (m, 1H); ^{13}C NMR (50 MHz, $CDCl_3$, 25 °C, TMS): $\delta=7.7$ (q), 14.1 (q), 22.7 (t), 26.1 (t), 31.7 (t), 34.6 (t), 36.7 (t), 46.6 (d), 48.3 (t), 52.1 (q), 156.7 (s), 210.7 ppm (s); elemental analysis calcd (%) for $C_{12}H_{23}NO_3$: C 62.85, H 10.11, N 6.11; found: C 62.59, H 10.05, N 6.14.

Compound ***5e*** *($C_{11}H_{21}NO_3$)*: Obtained from 7-methyl-4-octen-3-one (980 mg, 7 mmol), methylcarbamate (630 mg, 8.4 mmol), $(n\mathrm{Bu})_3$P (141.6 mg, 0.7 mmol), and TMSCl (837 mg, 7.7 mmol) as a colorless liquid (351 mg, 30 %); specific rotation of sample obtained from enzymatic kinetic resolution: $[\alpha]_D^{20}=+10.2$ ($c=0.60$ in $CHCl_3$; *ee* = 22 %); ^{1}H NMR (200 MHz, $CDCl_3$, 25 °C, TMS): $\delta=0.91$ (d, $J=6.4$ Hz, 6H), 1.03 (t, $J=6.6$ Hz, 3H), 1.20–1.27 (m, 1H), 1.41–1.72 (m, 2H), 2.41 (q, $J=7.2$ Hz, 2H), 2.62 (d, $J=3.6$ Hz, 2H), 3.63 (s, 3H), 3.89–4.05 (m, 1H), 5.04–5.11 ppm (m, 1H); ^{13}C NMR (50 MHz, $CDCl_3$, 25 °C, TMS): $\delta=7.7$ (q), 22.1 (q), 23.2 (q), 25.1 (d), 36.7 (t) 43.8 (d), 46.4 (t), 46.9 (t), 52.1 (q), 156.7 (s), 210.7 ppm (s); ESIMS-TOF (70 eV): *m*/*z* (%): 250 (100) $[M+2H_2O-H]^-$, 233 (60) $[M+H_2O]^-$, 204 (45) $[C_9H_{16}NO_3+H_2O]^-$, 190 (50) $[C_8H_{14}NO_3+H_2O]^-$, 181 (30) $[C_{10}H_{19}NO_3-H_2O-1]^-$, 154 (50) $[C_8H_{14}NO_3-H_2O]^-$, 139 (12) $[C_8H_{16}NO_2-H_2O-1]^-$.

Biotransformations: All biotransformations were conducted by using recombinant BVMOs from different bacterial origin expressed in *E. coli*. The following BVMOs were investigated for their substrate specificity towards linear aliphatic β-amino ketones: cyclohexanone monooxygenase from *A. calcoaceticus* NCIMB 9871 ($CHMO_{Acineto}$),[14] and seven other cyclohexanone monooxygenases ($CHMO_{Arthro}$ from *Arthrobacter sp.*,[63] $CHMO_{Brachy}$ from *Brachymonas sp.*,[64] $CHMO_{Brevi1}$ and $CHMO_{Brevi2}$ from *Brevibacterium sp.*,[65] $CHMO_{Rhodo1}$ and $CHMO_{Rhodo2}$ from *Rhodococcus sp.*,[63] and $CHMO_{Xantho}$ from *Xanthobacter sp.* ZL5[17]) as well as cyclopentanone monooxygenase (CPMO) from *Comamonas sp.* NCIMB 9872,[18] and cylododecanone monooxygenase (CDMO) from *Rhodococcus ruber* SC1.[20] Also arylketone-converting BVMOs 4-hydroxyacetophenone monooxygenase from *P. putida* JD1 ($HAPMO_{PpJD1}$),[21] 4-hydroxyacetophenone monooxygenase from *P. fluorescens* ACB ($HAPMO_{ACB}$),[22] and phenylacetone monooxygenase from *T. fusca* (PAMO)[28] have been investigated, followed by alkylketone-converting BVMOs from *P. putida* KT2440 ($BVMO_{PpKT2440}$),[24] *P. fluorescens* DSM 50106 ($BVMO_{Pfl}$),[23] and *M. tuberculosis* H37Rv ($BVMO_{Mtb5}$).[66] Because CPMO, $CHMO_{Brevi2}$, $HAPMO_{PpJD1}$, $BVMO_{PpKT2440}$, $BVMO_{Pfl}$, and BVMOMtb5 did not show activity against any substrate they were excluded from the results section.

Typical procedure for screening experiments: Analytical screening experiments were performed in 24-well plates. For this, precultures were inoculated with a single colony from a plate (LB_{amp}) and incubated at 37 °C overnight (or at 30 °C for CHMO from *Xanthobacter sp.*) in an orbital shaker in a baffled Erlenmeyer flask. After 20 h LB_{amp} (20 mL) was inoculated with 1 % of the overnight preculture and incubated at 37 and 30 °C, respectively, until OD_{600nm} reached 0.6–0.8 (usually after 3 h). Then, BVMO expression was induced with either IPTG (0.1 mM, final concentration) or in case of $HAPMO_{ACB}$ and PAMO with L-arabinose (0.2 % w/v, final concentration). Protein expression was performed at 24 °C for 2 h. Then, 1 mL of the bacterial culture was transferred into each well of the 24-well plate followed by subsequent substrate addition (1 mM, in dioxane). Biotransformations were carried out at 24 °C and analyzed after 24 h. Samples were extracted with ethyl acetate supplemented with 1 mM internal standard (benzoic acid methyl ester), dried over anhydrous sodium sulphate and examined by GC analysis.

Time-course experiments: Time-course experiments were performed as described for the screening experiments, with samples taken at definite time intervals (2, 4, 6, 8, 10, 24, 30, and 48 h).

Preparative-scale experiments: For preparative-scale experiments a baffled flask filled with LB_{amp} (500 mL) was inoculated with 1 % of the over-

night preculture and incubated at 37 °C in an orbital shaker. At OD_{600nm} 0.6–0.8 protein expression was induced with IPTG (0.1 mM) or L-arabinose (0.2 % w/v) followed by substrate addition (0.25 mmol, in dioxane). Protein expression and subsequent biotransformations were performed at 24 °C. At a conversion of about 50 % the whole volume was extracted four times with ethyl acetate (100 mL each). The organic layers were combined, dried over anhydrous sodium sulphate, and the organic solvent was evaporated. The crude product was purified by using silica-gel chromatography (petrol ether/ethyl acetate) and finally the amino ketone and the corresponding amino ester were analyzed by using GC, GCMS, and $^1H/^{13}C$ NMR.

Physical and spectral data of enzymatically synthesized N-protected β-amino esters

Compound ***2a*** *($C_{10}H_{19}NO_4$)*: Obtained enzymatically through biotransformation of **1a** (0.25 mmol, 51 mg) with $CHMO_{Brevi1}$ as a colorless liquid. Yield: 32 mg, 63 %; specific rotation of sample obtained from enzymatic kinetic resolution: $[\alpha]_D^{20} = -34.3$ ($c = 1.60$, in $CHCl_3$; $ee = 97\,\%$); ^1H NMR (200 MHz, $CDCl_3$, 25 °C, TMS): $\delta = 0.87$ (t, $J = 6.6$ Hz, 3H), 1.29–1.53 (m, 6H), 2.05 (s, 3H), 3.65 (s, 3H), 3.75–3.95 (m, 1H), 4.04 (d, $J = 4.5$ Hz, 2H), 4.66–4.79 ppm (m 1H); ^{13}C NMR (50 MHz, $CDCl_3$, 25 °C, TMS): $\delta = 13.9$ (q), 20.8 (q), 22.4 (t), 27.9 (t), 31.5 (t), 50.2 (d), 52.1 (q), 66.1 (t), 156.6 (s), 171.0 ppm (s).

Compound ***2c*** *($C_{12}H_{23}NO_4$)*: Obtained enzymatically through biotransformation of **1c** (0.25 mmol, 58 mg) with $CHMO_{Brevi1}$ as a colorless solid. Yield: 24 mg, 42 %; m.p. 61–63 °C; specific rotation of sample obtained from enzymatic kinetic resolution: $[\alpha]_D^{20} = -26.8$ ($c = 1.65$ in $CHCl_3$; $ee = 96\,\%$); ^1H NMR (200 MHz, $CDCl_3$, 25 °C, TMS): $\delta = 0.86$ (t, $J = 6.8$ Hz, 3H), 1.25–15.3 (m, 10H), 2.05 (s, 3H), 3.65 (s, 3H), 3.78–3.93 (m, 1H), 4.05 (d, $J = 4.7$ Hz, 2H), 4.64–4.78 ppm (m, 1H); ^{13}C NMR (50 MHz, $CDCl_3$, 25 °C, TMS): $\delta = 14.0$ (q), 20.8 (q), 22.5 (t), 25.7 (t), 29.0 (t), 31.6 (t), 31.8 (t), 50,2 (d), 52.1 (q), 66.1 (t), 156.6 (s), 171.0 ppm (s).

Compound ***2d*** *($C_{14}H_{27}NO_4$)*: Obtained enzymatically through biotransformation of **1d** (0.25 mmol, 65 mg) with $CHMO_{Brevi1}$ as a colorless solid. Yield: 3 mg, 5 %; m.p. 72–74 °C; specific rotation of sample obtained from enzymatic kinetic resolution: $[\alpha]_D^{20} = -25.3$ ($c = 0.15$ in $CHCl_3$; $ee = 98\,\%$); ^1H NMR (200 MHz, $CDCl_3$, 25 °C, TMS): $\delta = 0.88$ (t, $J = 6.6$ Hz, 3H), 1.16–1.55 (m, 14H), 2.07 (s, 3H), 3.67 (s, 3H), 3.77–3.93 (m, 1H), 4.06 (d, $J = 4.5$ Hz, 2H), 4.64–4.72 ppm (m, 1H); ^{13}C NMR (50 MHz, $CDCl_3$, 25 °C, TMS): $\delta = 14.1$ (q), 20.8 (q), 22.6 (t), 25.8 (t), 29.2 (t), 29.4 (t), 29.9 (t), 31.3 (t), 31.8 (t), 49.4 (d), 51.8 (q), 66.1 (t), 156.6 (s), 171.0 ppm (s).

Compound ***2e*** *($C_{10}H_{19}NO_4$)*: Obtained enzymatically through biotransformation of **1e** (0.25 mmol, 51 mg) with $CHMO_{Rhodo2}$ as a colorless liquid. Yield: 23 mg, 45 %; specific rotation of sample obtained from enzymatic kinetic resolution: $[\alpha]_D^{20} = -34.9$ ($c = 1.15$ in $CHCl_3$; $ee = 71\,\%$); ^1H NMR (200 MHz, $CDCl_3$, 25 °C, TMS): $\delta = 0.91$ (d, $J = 6.6$ Hz, 6H), 1.19–1.37 (m, 2H), 1.58–1.77 (m, 1H), 2.05 (s, 3H), 3.65 (s, 3H), 3.81–4.05 (m, 1H), 4.04 (d, $J = 4.7$ Hz, 2H), 4.67–4.72 ppm (m, 1H); ^{13}C NMR (50 MHz, CDCl, 25 °C, TMS): $\delta = 20.8$ (q), 23.0 (q), 23.0 (q), 24.6 (d), 40.9 (t), 48.4 (d), 52.1 (q), 66.6 (t), 156.6 (s), 171.0 ppm (s).

Compound ***2f*** *($C_9H_{17}NO_4$)*: Obtained enzymatically through biotransformation of **1f** (0.25 mmol, 47 mg) with $CHMO_{Rhodo2}$ as a colorless liquid. Yield: 18 mg, 38 %; specific rotation of sample obtained from enzymatic kinetic resolution: $[\alpha]_D^{20} = +22.8$ ($c = 0.90$ in $CHCl_3$; $ee = 43\,\%$); ^1H NMR (200 MHz, $CDCl_3$, 25 °C, TMS): $\delta = 0.93$ (dd, $J = 2.4$ Hz and 6.8 Hz, 6H), 1.72–1.89 (m, 1H), 2.05 (s, 3H), 3.66 (s, 3H), 3.68–3.75 (m, 1H), 4.08 (d, $J = 4.3$ Hz, 2H), 4.69–4.75 ppm (m, 1H); ^{13}C NMR (50 MHz, $CDCl_3$, 25 °C, TMS): $\delta = 18.3$ (q), 19.3 (q), 20.8 (q), 29.6 (d), 52.2 (q), 55.3 (d), 64.6 (t), 156.9 (s), 171.0 ppm (s).

Compound ***2g*** *($C_{12}H_{15}NO_4$)*: Obtained enzymatically through biotransformation of **1g** (0.25 mmol, 56 mg) with PAMO as a yellow liquid. Yield: 17 mg, 30 %; specific rotation of sample obtained in from enzymatic resolution: $[\alpha]_D^{20} = +26.4$ ($c = 0.85$ in $CHCl_3$; $ee = 99\,\%$); ^1H NMR (200 MHz, $CDCl_3$, 25 °C, TMS): $\delta = 2.05$ (s, 3H), 3.67 (s, 3H), 4.28 (d, $J = 5$ Hz, 2H), 4.93–5.09 (m, 1H), 5.28–5.39 (m, 1H), 7.25–7.36 ppm (m, 5H); ^{13}C NMR (50 MHz, $CDCl_3$, 25 °C, TMS): $\delta = 30.6$ (q), 48.9 (t), 51.4 (d), 52.2 (q), 126.2 (t), 126.2 (t), 127.5 (t), 128.6 (t), 128.6 (t), 141.2 (d), 156.3 (s), 206.8 ppm (s).

Compound ***6a*** *($C_{11}H_{21}NO_4$)*: Obtained enzymatically through biotransformation of **5a** (0.25 mmol, 54 mg) with CDMO as a colorless liquid. Yield: 3 mg, 6 %; specific rotation of sample obtained from enzymatic kinetic resolution: $[\alpha]_D^{20} = -24.4$ ($c = 0.15$ in $CHCl_3$; $ee = 99\,\%$); ^1H NMR (200 MHz, $CDCl_3$, 25 °C, TMS): $\delta = 0.92$ (t, $J = 6$ Hz, 3H), 1.17 (t, $J = 7.8$ Hz, 3H), 1.33–1.51 (m, 6H), 2.34 (q, $J = 7.8$ Hz, 2H), 3.67 (s, 3H), 4.10–4.18 (m, 1H), 4.13–4.21 (m, 2H), 4.65 ppm (m, 1H); ^{13}C NMR (50 MHz, $CDCl_3$, 25 °C, TMS): $\delta = 9.1$ (q), 14.1 (q), 22.7 (t), 27.8 (t), 29.7 (t), 31.9 (t), 49.4 (d), 52.5 (q), 66.7 (t), 156.6 (s), 174.2 ppm (s).

Compound ***6b*** *($C_{12}H_{23}NO_4$)*: Obtained enzymatically through biotransformation of **5b** (0.25 mmol, 58 mg) with CDMO as a colorless solid. Yield: 10 mg, 17 %; m.p. 53–55 °C; specific rotation of sample obtained from enzymatic kinetic resolution: $[\alpha]_D^{20} = -26.5$ ($c = 0.50$, $CHCl_3$; $ee = 84\,\%$); ^1H NMR (200 MHz, $CDCl_3$, 25 °C, TMS): $\delta = 0.88$ (t, $J = 6.6$ Hz, 3H), 1.14 (t, $J = 7.6$ Hz, 3H), 1.23–1.45 (m, 8H), 2.34 (q, $J = 7.6$ Hz, 2H), 3.66 (s, 3H), 3.78–3.95 (m, 1H), 4.09 (d, $J = 7.2$ Hz, 2H), 4.62–4.71 ppm (m, 1H); ^{13}C NMR (50 MHz, $CDCl_3$, 25 °C, TMS): $\delta = 9.1$ (q), 14.0 (q), 22.5 (t), 25.4 (t), 27.5 (t), 31.5 (t), 31.8 (t), 50.3 (d), 52.1 (q), 66.0 (t), 156.6 (s), 174.4 ppm (s).

Compound ***7e*** *($C_{11}H_{21}NO_4$)*: Obtained enzymatically through biotransformation of **5e** (0.25 mmol, 54 mg) with CDMO as a colorless liquid. Yield: 3 mg, 6 %; specific rotation of sample obtained from enzymatic kinetic resolution: $[\alpha]_D^{20} = +19.6$ ($c = 0.15$ in $CHCl_3$; $ee = 99\,\%$); ^1H NMR (200 MHz, $CDCl_3$, 25 °C, TMS): $\delta = 0.89$ (d, $J = 6.6$ Hz, 6H), 1.28 (t, $J = 7.2$ Hz, 3H), 1.40–1.47 (m, 2H), 1.53–1.68 (m, 1H), 2.51 (d, $J = 4.8$ Hz, 2H), 3.65 (s, 3H), 4.02–4.16 (m, 1H), 4.14 (q, $J = 7.2$ Hz, 2H), 4.98–5.07 ppm (m, 1H); ^{13}C NMR (50 MHz, $CDCl_3$, 25 °C, TMS): $\delta = 14.2$ (q), 22.1 (q), 22,9 (q), 24.9 (d), 39.2 (d), 39.5 (t), 44.8 (t), 52.7 (q), 60.5 (t), 156.4 (s), 170.2 ppm (s).

Computer modeling: Computer modeling studies were performed by using YASARA structure (version 9.7.24) and the AMBER03 force field with default settings.[67] AutoSMILES force field assignment was used for cofactors and substrates.[68] To get an active model of PAMO (pdb-code: 1W4X[56]) the missing $NADP^+$ was taken from a homologous cyclohexanone monooxygenase from *Rhodococcus* HI-31 (pdb-code: 3GWF[58]) after structural alignments by using the MUSTANG algorithm.[68] Energy minimization was performed in a periodic water box at pH 7.0. Substrates were docked into the active site by using Autodock4 and the Lamarckian genetic algorithm[70] with max 50 million energy evaluations, max 60000 generations and default parameters. Analysis was carried out by using YASARA structure. For visualization PyMol (DeLano Scientific, Palo Alto, CA, USA.; http://www.PyMol.org) was used.

Acknowledgements

The authors thank the Deutsche Bundesstiftung Umwelt (DBU, AZ 80006/871) for a scholarship to J.R. and the Austrian Science Fund FWF (Project No. 18945). Furthermore, we thank Dr. Qiong Cheng and Dr. Pierre Rouviere (DuPont USA) as well as Dr. Jan B. van Beilen (formerly ETH Zürich, now Université de Lausanne, Switzerland) for generously providing recombinant expression systems for BVMOs used in this work.

[1] G.-J. ten Brink, I. W. C. E. Arends, R. A. Sheldon, *Chem. Rev.* **2004**, *104*, 4105–4124.
[2] M. Renz, B. Meunier, *Eur. J. Org. Chem.* **1999**, 737–750.
[3] G. R. Krow, *Org. React.* **1993**, *43*, 251–296.
[4] A. von Baeyer, V. Villiger, *Ber. Dtsch. Chem. Ges.* **1899**, *32*, 3625–3633.
[5] G. E. Turfitt, *Biochem. J.* **1948**, *42*, 376–383.
[6] G. Strukul, A. Varagnolo, F. Pinna, *J. Mol. Catal. A* **1997**, *117*, 413–423.
[7] A. Gusso, C. Baccin, F. Pinna, G. Strukul, *Organometallics* **1994**, *13*, 3442–3451.
[8] C. M. Clouthier, M. M. Kayser, M. T. Reetz, *J. Org. Chem.* **2006**, *71*, 8431–8437.

[9] M. D. Mihovilovic, F. Rudroff, A. Winninger, T. Schneider, F. Schulz, M. T. Reetz, *Org. Lett.* **2006**, *8*, 1221–1224.
[10] M. Bocola, F. Schulz, F. Leca, A. Vogel, M. W. Fraaije, M. T. Reetz, *Adv. Synth. Catal.* **2005**, *347*, 979–986.
[11] M. T. Reetz, B. Brunner, T. Schneider, F. Schulz, C. M. Clouthier, M. M. Kayser, *Angew. Chem.* **2004**, *116*, 4167–4170; *Angew. Chem. Int. Ed.* **2004**, *43*, 4075–4078.
[12] N. M. Kamerbeek, D. B. Janssen, W. J. H. van Berkel, M. W. Fraaije, *Adv. Synth. Catal.* **2003**, *345*, 667–678.
[13] J. Rehdorf, U. T. Bornscheuer in *Encyclopedia of Industrial Biotechnology: Bioprocess, Bioseparation, and Cell Technology* (Ed.: M. C. Flickinger), Wiley, **2010**, DOI: 10.1002/9780470054581.eib451.
[14] Y.-C. J. Chen, O. P. Peoples, C. T. Walsh, *J. Bacteriol.* **1988**, *170*, 781–789.
[15] M. D. Mihovilovic, B. Müller, P. Stanetty, *Eur. J. Org. Chem.* **2002**, 3711–3730.
[16] M. D. Mihovilovic, *Curr. Opin. Chem.* **2006**, *10*, 1265–1287.
[17] J. B. van Beilen, F. Mourlane, M. A. Seeger, J. Kovac, Z. Li, T. H. M. Smits, U. Fritsche, B. Witholt, *Environ. Microbiol.* **2003**, *5*, 174–182.
[18] H. Iwaki, Y. Hasegawa, S. Wang, M. M. Kayser, P. C. K. Lau, *Appl. Environ. Microbiol.* **2002**, *68*, 5671–5684.
[19] H. Iwaki, S. Wang, S. Grosse, H. Bergeron, J. Nagahashi, J. Lertvorachon, J. Yang, Y. Konishi, Y. Hasegawa, P. C. K. Lau, *Appl. Environ. Microbiol.* **2006**, *72*, 2707–2720.
[20] K. Kostichka, S. M. Thomas, K. J. Gibson, V. Nagarajan, Q. Cheng, *J. Bacteriol.* **2001**, *183*, 6478–6486.
[21] J. Rehdorf, C. L. Zimmer, U. T. Bornscheuer, *Appl. Environ. Microbiol.* **2009**, *75*, 3106–3114.
[22] N. M. Kamerbeek, M. J. H. Moonen, J. G. M. van der Ven, W. J. H. van Berkel, M. W. Fraaije, D. B. Janssen, *Eur. J. Biochem.* **2001**, *268*, 2547–2557.
[23] A. Kirschner, J. Altenbuchner, U. T. Bornscheuer, *Appl. Microbiol. Biotechnol.* **2006**, *73*, 1065–1075.
[24] J. Rehdorf, A. Kirschner, U. T. Bornscheuer, *Biotechnol. Lett.* **2007**, *29*, 1393–1398.
[25] A. Völker, A. Kirschner, U. T. Bornscheuer, J. Altenbuchner, *Appl. Microbiol. Biotechnol.* **2008**, *77*, 1251–1260.
[26] L. N. Britton, A. J. Markovetz, *J. Biol. Chem.* **1977**, *252*, 8561–8566.
[27] N. M. Kamerbeek, J. J. Olsthoorn, M. W. Fraaije, D. B. Janssen, *Appl. Environ. Microbiol.* **2003**, *69*, 419–426.
[28] M. W. Fraaije, J. Wu, D. P. H. M. Heuts, E. W. van Hellemond, J. H. Lutje Spelberg, D. B. Janssen, *Appl. Microbiol. Biotechnol.* **2005**, *66*, 393–400.
[29] J. Rehdorf, A. Lengar, U. T. Bornscheuer, M. D. Mihovilovic, *Bioorg. Med. Chem. Lett.* **2009**, *19*, 3739–3743.
[30] A. Kirschner, U. T. Bornscheuer, *Angew. Chem.* **2006**, *118*, 7161–7163; *Angew. Chem. Int. Ed.* **2006**, *45*, 7004–7006; *Angew. Chem.* **2006**, *118*, 7161–7163.
[31] J. Rehdorf, M. D. Mihovilovic, U. T. Bornscheuer, *Angew. Chem. Int. Ed.* **2010**, *49*, 4506–4507; *Angew. Chem.* **2010**, *122*, 4609–4611.
[32] Shivani, B. Pujala, A. K. Chakraborti, *J. Org. Chem.* **2007**, *72*, 3713–3722.
[33] N. Azizi, M. R. Saidi, *Org. Lett.* **2005**, *7*, 3649–3651.
[34] A. Heydari, M. Mehrdad, A. Maleki, N. Ahmadi, *Synthesis* **2004**, 1557–1558.
[35] D. Menche, F. Arikan, J. Li, S. Rudolph, *Org. Lett.* **2007**, *9*, 267–270.
[36] G. Liu, S. S. Stahl, *J. Am. Chem. Soc.* **2006**, *128*, 7179–7181.
[37] M. Kitamura, O. Takeshi, I. Shinichi, N. Sayo, H. Kumobayashi, S. Akutagawa, T. Ohta, H. Takaya, R. Noyori, *J. Am. Chem. Soc.* **1988**, *110*, 629–631.
[38] L. Dahlenburg, H. Treffert, F. Christian, F. W. Heinemann, A. Zahl, *Eur. J. Inorg. Chem.* **2007**, 1738–1751.
[39] J. V. Potetinova, T. L. Voyushina, V. M. Stepanov, *Bioorg. Med. Chem. Lett.* **1997**, *7*, 705–710.
[40] G. Sekar, R. M. Kamble, V. K. Singh, *Tetrahedron: Asymmetry* **1999**, *10*, 3663–3666.
[41] M. D. Mihovilovic, B. Müller, M. M. Kayser, J. D. Stewart, J. Fröhlich, P. Stanetty, H. Spreitzer, *J. Mol. Catal. B* **2001**, *11*, 349–353.
[42] L.-W. Xu, C.-G. Xia, *Tetrahedron Lett.* **2004**, *45*, 4507–4510.
[43] T. Kourouli, P. Kefalas, N. Ragoussis, V. Ragoussis, *J. Org. Chem.* **2002**, *67*, 4615–4618.
[44] M. M. Kayser, G. Chen, J. D. Stewart, *Synlett* **1999**, 153–158.
[45] M. D. Mihovilovic, R. Snajdrova, A. Winninger, F. Rudroff, *Synlett* **2005**, 2751–2754.
[46] C.-S. Chen, Y. Fujimoto, G. Girdaukas, C. J. Sih, *J. Am. Chem. Soc.* **1982**, *104*, 7294–7299.
[47] K. Faber, H. Hönig, A. Kleewein Free shareware programs (Selectivity-1.0) for calculation of the enantiomeric ratio; ftp://borgc185.kfunigraz.ac.at/pub/enantio/.
[48] M. D. Mihovilovic, F. Rudroff, B. Grötzl, P. Kapitan, R. Snajdrova, J. Rydz, *Angew. Chem.* **2005**, *117*, 3675–3679; *Angew. Chem. Int. Ed.* **2005**, *44*, 3609–3613.
[49] F. Rudroff, J. Rydz, F. J. Ogink, M. Fink, M. D. Mihovilovic, *Adv. Synth. Catal.* **2007**, *349*, 1436–1444.
[50] R. Snajdrova, G. Grogan, M. D. Mihovilovic, *Bioorg. Med. Chem. Lett.* **2006**, *16*, 4813–4817.
[51] M. D. Mihovilovic, P. Kapitán, P. Kapitánová, *ChemSusChem* **2008**, *1*, 143–148.
[52] P. Cernuchová, M. D. Mihovilovic, *Org. Biomol. Chem.* **2007**, *5*, 1715–1719.
[53] V. Alphand, R. Furstoss, *J. Org. Chem.* **1992**, *57*, 1306–1309.
[54] F. Petit, R. Furstoss, *Tetrahedron: Asymmetry* **1993**, *4*, 1341–1352.
[55] A. Rioz-Martínez, G. de Gonzalo, D. E. Torres-Pazmiño, M. W. Fraaije, V. Gotor, *Eur. J. Org. Chem.* **2009**, 2526–2523.
[56] C. Rodríguez, G. de Gonzalo, M. W. Fraaije, V. Gotor, *Tetrahedron: Asymmetry* **2007**, *18*, 1338–1344.
[57] E. Malito, A. Alfieri, M. W. Fraaije, A. Mattevi, *Proc. Natl. Acad. Sci. USA* **2004**, *101*, 13157–13162.
[58] I. A. Mirza, B. J. Yachin, S. Wang, S. Grosse, H. Bergeron, A. Imura, H. Iwaki, Y. Hasegawa, P. C. Lau, A. M. Berghuis, *J. Am. Chem. Soc.* **2009**, *131*, 8848–8854.
[59] F. Schulz, F. Leca, F. Hollmann, M. T. Reetz, *Beilstein J. Org. Chem.* **2005**, *1*, 1–10.
[60] M. T. Reetz, M. Bocola, J. D. Carballeira, D. Zha, A. Vogel, *Angew. Chem.* **2005**, *117*, 4264–4268; *Angew. Chem. Int. Ed.* **2005**, *44*, 4192–4196.
[61] M. T. Reetz, D. Kahakeaw, J. Sanchis, *J. Mol. Biosyst.* **2009**, *5*, 115–122.
[62] M. T. Reetz, S. Wu, *J. Am. Chem. Soc.* **2009**, *131*, 15424–15432.
[63] P. C. Brzostowicz, D. M. Walters, S. M. Thomas, V. Nagarajan, P. E. Rouvière, *Appl. Environ. Microbiol.* **2003**, *69*, 334–342.
[64] M. G. Bramucci, P. C. Brzostowicz, K. Kostichka, V. Nagarajan, P. E. Rouvière, S. M. Thomas, PCT International Application, **2003**, WO 2003020890 [*Chem. Abstr* **2003**, *138*, 233997].
[65] P. C. Brzostowicz, K. L. Gibson, S. M. Thomas, M. S. Blasko, P. E. Rouvière, *J. Bacteriol.* **2000**, *182*, 4241–4248.
[66] D. Bonsor, S. F. Butz, J. Solomons, S. Grant, I. J. S. Fairlamb, M. J. Fogg, G. Grogan, *Org. Biomol. Chem.* **2006**, *4*, 1252–1260.
[67] E. Krieger, T. Darden, S. Nabuurs, A. Finkelstein, G. Vriend, *Proteins* **2004**, *57*, 678–683.
[68] A. Jakalian, D. B. Jack, C. I. Bayly, *J. Comput. Chem.* **2002**, *23*, 1623–1641.
[69] A. S. Konagurthu, J. C. Whisstock, P. J. Stuckey, A. M. Lesk, *Proteins* **2006**, *64*, 559–574.
[70] G. M. Morris, D. S. Goodsell, R. S. Halliday, R. Huey, W. E. Hart, R. K. Belew, A. J. Olson, *J. Comput. Chem.* **1998**, *19*, 1639–1662.

Received: May 28, 2010
Published online: July 21, 2010

